

Ab initio lattice results for Fermi polarons in two and three dimensions

Shahin Bour,¹ Dean Lee,² H.-W. Hammer,^{3,4} and Ulf-G. Meißner^{1,5}

¹*Helmholtz-Institut für Strahlen- und Kernphysik (Theorie)*

and Bethe Center for Theoretical Physics, Universität Bonn, 53115 Bonn, Germany

²*Department of Physics, North Carolina State University, Raleigh, NC 27695, USA*

³*Institut für Kernphysik, Technische Universität Darmstadt, D-64289 Darmstadt, Germany*

⁴*ExtreMe Matter Institute EMMI, GSI Helmholtzzentrum für Schwerionenforschung GmbH, D-64291 Darmstadt, Germany*

⁵*Institut für Kernphysik, Institute for Advanced Simulation and Jülich Center for Hadron Physics, Forschungszentrum Jülich, D-52425 Jülich, Germany*

We investigate the attractive Fermi polaron problem in two and three dimensions using non-perturbative Monte Carlo simulations. We introduce a new Monte Carlo algorithm called the impurity lattice Monte Carlo method. This algorithm samples the path integral in a computationally efficient manner and has only small sign oscillations for systems with a single impurity. To benchmark the method, we calculate the universal polaron energy in three dimensions in the scale-invariant unitarity limit and find agreement with published results. We then present the first fully non-perturbative calculations of the polaron energy in two dimensions in the limit of zero range interactions. We find evidence for a smooth crossover transition from a fermionic quasiparticle to a molecular state as a function of interaction strength with significant mixing between the two descriptions in the crossover region.

PACS numbers: 67.85.Lm, 02.70.Ss, 71.38.-k

One of the most interesting and fundamental problems in quantum many-body physics is the polaron problem, where a mobile impurity interacts with a bath of particles. With the advent of trapped ultracold atomic gases, the polaron problem can now be realized for both bosonic and fermionic baths, and also in the universal limit where the range of the particle interactions is negligible [1]. In a fermionic medium, the impurity can undergo a transition and change its quantum statistics by binding fermions from the surrounding Fermi gas [2, 3]. The impurity is dressed by fluctuations of the Fermi sea forming a quasiparticle or polaron state. But with increasing particle interaction strength, molecules will form by capturing one or even two particles from the Fermi sea. This behavior has been shown to depend on the mass ratio of the two components of the Fermi gas for the 3D case [2–10]. In 1D the exact analytical solution shows that there is no polaron-molecule transition [11]. In 2D the Fermi polaron properties have been studied using different theoretical and experimental approaches, and these have predicted various scenarios for the existence or absence of a polaron-molecule transition [12–20]. The Fermi polaron system has been studied using diagrammatic Monte Carlo (diag MC) [19–21]. The diag MC method uses a worm algorithm to stochastically sample Feynman diagrams to high orders in the coupling constant.

In this work, we introduce a non-perturbative *ab initio* approach called impurity lattice Monte Carlo (ILMC) [22] to investigate highly imbalanced Fermi gases in 2D and 3D. Unlike diag MC, impurity lattice Monte Carlo directly samples the path integral rather than relying on a perturbative diagrammatic expansion. Therefore it is a fully non-perturbative calculation that can probe the transition from polaron or fermionic quasiparticle to

molecule state and shed light on the transition where there may be mixing between the two. Furthermore, the method can easily be extended to study impurities in paired superfluids.

Impurity lattice Monte Carlo method. The impurity lattice Monte Carlo method is a hybrid of two Monte Carlo algorithms, namely, worldline and auxiliary-field Monte Carlo (AFMC) algorithms. In the ILMC approach, the spacetime worldlines of each impurity are sampled explicitly while all other particles are handled using the auxiliary-field formalism. The impurity worldlines also function as local auxiliary fields felt by the other particles in the system.

We illustrate the method by considering a d -dimensional many-body system of two-component fermions with equal masses, $m_{\uparrow} = m_{\downarrow} = m$ and attractive interactions in the zero-range limit. In our many-body system N up-spin particles fill the Fermi sea and one down-spin particle acts as an impurity immersed in this Fermi sea. In the zero-range limit, the interaction potential can be replaced by a delta function interaction. Using the lattice spacing to regularize the short distance physics, we can write our lattice Hamiltonian as

$$H = H_0 + C_0 \sum_{\vec{n}} a_{\uparrow}^{\dagger}(\vec{n}) a_{\uparrow}(\vec{n}) a_{\downarrow}^{\dagger}(\vec{n}) a_{\downarrow}(\vec{n}), \quad (1)$$

where \vec{n} denote spatial lattice points on a d -dimensional periodic hypercube of volume L^d . The free lattice Hamiltonian H_0 is given by

$$H_0 = H_0^{\uparrow} + H_0^{\downarrow} =$$

$$\frac{-\hbar^2}{2ma^2} \sum_{\mu=1}^d \sum_{\vec{n}, i=\uparrow, \downarrow} a_i^\dagger(\vec{n}) [a_i(\vec{n} + \hat{\mu}) - 2a_i(\vec{n}) + a_i(\vec{n} - \hat{\mu})], \quad (2)$$

where a is the spatial lattice spacing. We fix the coupling constant C_0 in order to reproduce either the desired two-particle scattering length or the binding energy of a shallow dimer at infinite volume. The partition function of the system can be written as

$$\mathcal{Z} = \text{Tr}(M^{L_t}), \quad (3)$$

where M is the normal-ordered transfer matrix operator

$$M =: \exp \left\{ \frac{-a_t}{\hbar} \left[H_0 + C_0 \sum_{\vec{n}} a_\uparrow^\dagger(\vec{n}) a_\uparrow(\vec{n}) a_\downarrow^\dagger(\vec{n}) a_\downarrow(\vec{n}) \right] \right\} :, \quad (4)$$

and a_t is the temporal lattice spacing.

We are interested in the system containing one down-spin particle together with N up-spin particles. Let us consider one forward time step from n_t to $n_t + 1$. If the down-spin worldline remains stationary at some lattice site \vec{n} during this time step, then there is an interaction between the impurity and the up spins. We get an effective transfer matrix for the up-spin particles that has the form

$$M_\uparrow(n_t) = \left(1 - \frac{da_t \hbar}{ma^2} \right) \times : \exp \left\{ \frac{-a_t}{\hbar} \left[H_0^\uparrow + \frac{C_0}{1 - \frac{da_t \hbar}{ma^2}} \rho_\uparrow(\vec{n}) \right] \right\} :. \quad (5)$$

We note the local potential generated by the down-spin impurity sitting at lattice site \vec{n} . If the down-spin worldline instead hops from one spatial lattice site to another, then there is no interaction between the impurity and the up spins. Therefore the effective up-spin transfer matrix is

$$M_\uparrow(n_t) = \left(\frac{a_t \hbar}{2ma^2} \right) : \exp \left\{ \frac{-a_t}{\hbar} H_0^\uparrow \right\} :. \quad (6)$$

For more details on the impurity lattice Monte Carlo formalism, we refer to Ref. [22].

Polarons in three dimensions at unitarity. As a benchmark of the ILMC method, we present simulations of polarons in the 3D unitarity limit. We define $\epsilon_p < 0$ as the difference between ground state energy of the system with a single impurity compared to the system without the impurity. In the unitarity limit, where the S -wave scattering length diverges, the polaron energy is a universal quantity and scales with the Fermi energy, $\epsilon_p = \theta \epsilon_F$, where θ is a universal dimensionless number.

Using our effective up-spin transfer matrix, we compute Euclidean time projection amplitudes of the form

$$\mathcal{Z}(L_t) = \langle \Psi_{\text{init}} | M_\uparrow(L_t - 1) \cdots M_\uparrow(0) | \Psi_{\text{init}} \rangle, \quad (7)$$

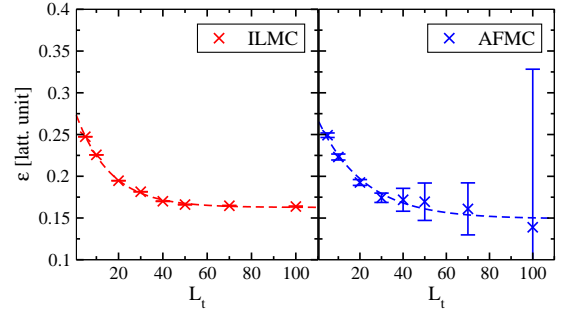


FIG. 1: (Color online) The ground state energy as a function of Euclidean projection time for ILMC simulations versus AFMC simulations for $L^3 = 10^3$ and $N = 10$.

where $|\Psi_{\text{init}}\rangle$ is a Slater-determinant initial wave function for the up spins. The amplitude for N up spins is given by the determinant of the $N \times N$ matrix of amplitudes for the single-particle initial wave functions.

We determine the ground state energy by taking the ratio of projection amplitudes for L_t and $L_t - 1$ time steps in the limit of large L_t . In order to do this extrapolation, we fit the ratio of the projection amplitude to the asymptotic exponential function $\epsilon_0 + \alpha e^{-\delta \cdot t}$ and determine the ground state energy ϵ_0 for each system at fixed particle number and volume.

In Fig. 1, we show a sample of the ILMC results for an $L^3 = 10^3$ lattice with $N = 10$. For comparison, we show the results that one obtains using AFMC calculations where all particles are treated using auxiliary fields. It is clear that the ILMC results are far better than the AFMC results. The reasons for this are twofold. First of all, the ILMC simulations are computationally simpler and run much faster than the AFMC simulations. But the main difference is that the ILMC simulations have far smaller sign oscillations compared with the AFMC simulations. We discuss the underlying reasons for this suppression of sign oscillations later in our discussion.

In order to determine the polaron energy at unitarity, we have performed simulations for several different lattice volumes L^3 as well as several different values for N , the number of up-spin particles. Since the scattering length is tuned to infinity, taking the limit of infinite volume at fixed particle number corresponds to taking the continuum limit with the interaction range going to zero. At fixed particle number, we determine the polaron energy for each system at lattice volumes 6^3 , 7^3 , 8^3 , 9^3 and 10^3 . We then apply a linear extrapolation in the inverse lattice spacing, the expected leading lattice-spacing dependence of corrections from the scale-invariant unitarity limit. See for example Ref. [23] for similar extrapolations in the unitarity limit. Repeating this procedure for systems with $N = 15, 20, 25, 30$ and 35 , we also extrapolate the polaron energy to the thermodynamic limit. For the thermodynamic limit extrapolation, we perform a linear fit in $1/N$.

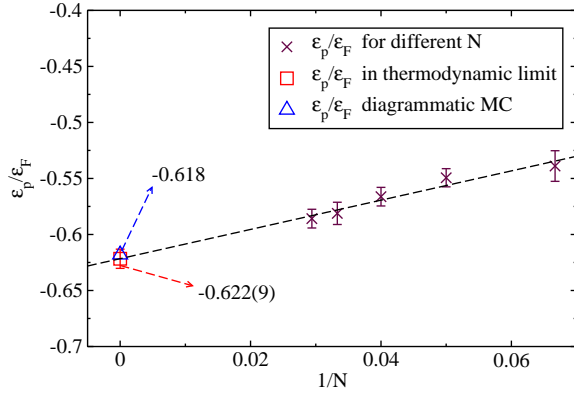


FIG. 2: (Color online) The 3D unitarity limit polaron energy ϵ_p in units of the Fermi energy ϵ_F as a function of the inverse particle number $1/N$. The square is the ILMC result in thermodynamic limit, while the triangle gives the diagrammatic Monte Carlo result from Ref. [2].

In Fig. 2, we show results for the polaron energy in the unitarity limit. Using the impurity lattice Monte Carlo method, we find $\theta = \epsilon_p/\epsilon_F = -0.622(9)$. This result is in very good agreement with the result $\theta = -0.618$ determined in Ref. [2] using diagrammatic Monte Carlo calculations and with the variational calculations with one and two particle-hole pair excitations giving $\theta = -0.6066$ [24] and $\theta = -0.6158$ [7], respectively. All these theoretical calculations are also consistent with the experimental values $\theta = -0.58(5)$ [25] and $\theta = -0.64(7)$ [10] measured in ultracold atomic gases.

Attractive polarons in two dimensions. We now consider attractive polarons in two dimensions. There is no analog of the unitarity limit in two dimensions since the only scale-invariant fixed point is in the weakly interacting limit [26, 27]. But there is a very interesting and important question as to whether a polaron-molecule transition occurs in the ground state as a function of the interaction strength. At this time experiments are not yet conclusive on the question of a transition [16, 17]. The possible existence and nature of such a transition impacts the overall phase diagram for spin-imbalanced 2D Fermi gas [28–32]. Some work using a variational approach did not show any ground-state transition [12]. However later studies found evidence for a transition when treating molecule and polaron variational wave functions in a similar fashion [14], and similar findings have been obtained in diagrammatic Monte Carlo simulations [19, 20]. While these variational and diag MC studies are impressive and informative, one does not gain information about the nature of the transition itself. Separate calculations are needed to describe the fermionic polaron and the molecular state, and there is no overlapping region where both calculations are reliable. In order to remedy this situation, we use impurity lattice Monte Carlo simulations to study the non-perturbative physics of the transition in detail.

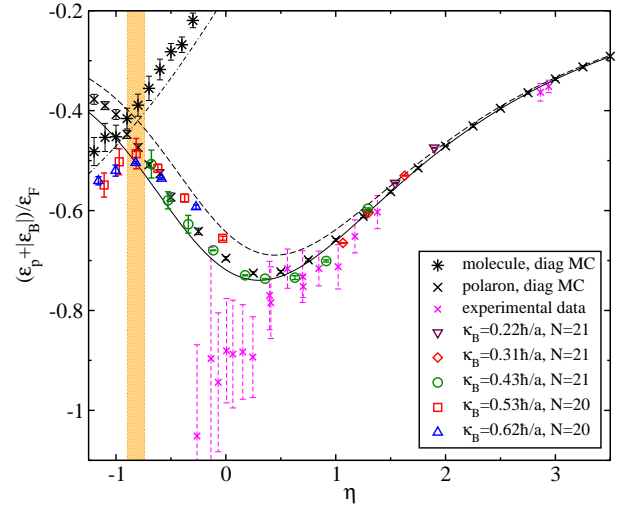


FIG. 3: (Color online) Ground state energy as a function of the dimensionless parameter $\eta \equiv \frac{1}{2} \ln \left(\frac{2\epsilon_F}{|\epsilon_B|} \right)$ in comparison with diag MC results [19]. The experimental data is from Ref. [33]. Dashed line: polaron variational results using one particle-hole (p-h) pair [14]. Solid line: polaron variational results using up to two p-h pairs [18]. Dot-dashed line: improved molecule state variational results including one p-h pair [14]. The vertical band represents the region where the crossover transition from polaron to molecule occurs.

We consider again one spin-down impurity and N spin-up particles in the limit of zero-range attractive interactions. The delta function interaction is tuned according to the two-body bound state energy, $|\epsilon_B|$. Using impurity lattice Monte Carlo, we calculate the polaron energy as a fraction of the up-spin Fermi energy. We tune the coupling constant in order to get the two-body bound states with binding momentum $\kappa_B = \sqrt{m|\epsilon_B|}$ equal to $0.22\hbar/a$, $0.31\hbar/a$, $0.43\hbar/a$, $0.53\hbar/a$, and $0.62\hbar/a$.

We run simulations for several different lattice areas, L^2 , and several different particle numbers, N . The lattice sizes go from $L^2 \times L_t = 20^2 \times 100$ to $L^2 \times L_t = 80^2 \times 700$. For each L^2 and N we find the ground state energy by extrapolating to the limit $L_t \rightarrow \infty$ by fitting the Euclidean time projection amplitude to the asymptotic function $\epsilon_0 + \alpha e^{-\delta \cdot t}$. To magnify the details we subtract the dimer energy in vacuum, ϵ_B , from the polaron energies and scale by ϵ_F , the majority up-spin particle Fermi energy.

In Fig. 3, we have plotted the subtracted-scaled polaron energy $(\epsilon_p + |\epsilon_B|)/\epsilon_F$ versus the dimensionless parameter $\eta \equiv \frac{1}{2} \ln \left(\frac{2\epsilon_F}{|\epsilon_B|} \right)$, which characterizes the strength of the interaction. The simulations are done with $N = 21$ and $N = 20$ up-spin particles. For comparison, we have plotted the diagrammatic Monte Carlo results from Ref. [19] and variational results from Ref. [14] and [18]. The dashed line shows polaron variational results including one particle-hole (p-h) pair [14], and the solid line gives polaron variational results including up to two p-h pairs [18]. The dot-dashed line shows the improved vari-

ational results for the molecule state including one p-h pair [14]. We also compare with experimental data [33] presented in Ref. [16] and find good agreement for the weak-coupling region, $\eta > 1$. For the strong coupling region, $\eta < 1$, the experimental uncertainty increases dramatically and there seem to be non-universal systematic effects in the experimental realization that need to be corrected (see for example Ref. [34]).

We see that for $\eta > -0.75$ the ILMC results are in excellent agreement with the fermionic polaron results obtained using diagrammatic Monte Carlo and two particle-hole variational calculations. For $\eta < -0.90$, the lattice results have a similar track as the diagrammatic Monte Carlo and variational results for the molecular state. But in this case, the lattice energies lie below the diag MC results. This may be an indication that the non-perturbative ground wave function is a mixture of polaron and molecular components. In the very strong coupling limit $\eta \rightarrow -\infty$, one expects $(\epsilon_p + |\epsilon_B|)/\epsilon_F$ to approach -1 from above. This corresponds to a tightly-bound molecule that has pulled one up-spin from the Fermi sea and is only weakly repelled by the remaining up spins.

Perhaps most interesting is that the lattice results show a smooth dependence on energy in the intermediate region $-0.90 < \eta < -0.75$. We interpret this as evidence for a smooth crossover from fermionic polaron to bosonic molecular state with significant mixing between polaron and molecular components. We can obtain further information about this transition from the dependence on the initial state wave functions.

In the weak coupling regime, we find that the convergence to the ground state is fastest when we use an initial state consisting of a Slater determinant of non-interacting fermions. In the strong coupling regime, the convergence to the ground state is enhanced when we use an initial state where the up-spin wave function consists of a Gaussian wave packet for one up-spin particle centered around the down-spin impurity, while the rest are $N - 1$ free fermions. The initial position of the impurity is summed over all possible coordinates to make a translationally-invariant state. These two distinct optimal initial states for the weak and strong coupling limits are a clear indicator of a transition from fermionic polaron to paired molecular state as a function of coupling strength.

Despite the computational advantages of one initial state over another, we can also obtain the same ground state energies within error bars using different initial states. The paired Gaussian wave packet initial state does well for simulations far into the weak coupling limit when we change the size of the wave packet. At strong coupling, the optimal wave packet is fairly compact, indicating a localized pair. At weak coupling, the optimal wave packet is very large, growing as big as the lattice length L . If we take this to be a measure of pair size,

then in the crossover transition region the pair size is comparable to the average separation distance between up spins.

The location of our crossover region is in good agreement with the results of diag MC calculations which have found transitions at $\eta = -0.95 \pm 0.15$ [19] and $\eta = -1.1 \pm 0.2$ [20]. This result is also consistent with variational calculations [18] which obtains a transition in the region $-0.97 < \eta < -0.80$. Our result also compares well with the experimental result, $\eta = -0.88(20)$, obtained after converting the experimental data [33] performed in a quasi-2D trap to their corresponding pure 2D values [34].

We have done simulations for a wide range of particle numbers and found very rapid convergence to the thermodynamic limit $N \rightarrow \infty$. In fact we find very little dependence on N for $N \geq 8$. The lattice results in Fig. 3 correspond to simulations with the largest numbers of particles, $N = 21$ for weak coupling and $N = 20$ for strong coupling. As we can see in Fig. 3, there is also relatively little spread in the lattice results for different values of the binding momenta. This indicates that we are close to the continuum limit of zero-range interactions, and so corrections to continuum limit are numerically small. In future work, we will perform additional simulations and do the thermodynamic and continuum limit extrapolations explicitly.

In all of the lattice simulations presented here we have found that, with a sensible choice of initial state, the sign oscillations are mild and have little impact on the quality of the simulations. This is good news for large scale ILMC simulations of other systems. Some possible examples include alpha particles in dilute neutron gases, Λ hyperons in neutron and nuclear matter, imbalanced cold atomic systems, and Kondo spin impurities. In these simulations one uses auxiliary-field Monte Carlo simulations for the majority particles in addition to the impurity worldline updates. If the simulations without the impurity can be done, then simulations with the impurity can also be done with little increase in sign oscillations.

At weak coupling, we find that the impurity worldline has only a minor effect on the eigenvalues of the $N \times N$ matrix of single-particle amplitudes, and so the determinant of the matrix remains positive. At strong coupling, we find one large positive eigenvalue that fluctuates in size depending on the impurity worldline. But this large eigenvalue is positive and the other eigenvalues once again are largely independent of the worldline. So the determinant remains positive in this case also. This seems to reflect the underlying physics that at strong coupling, we have a tightly-bound molecule which interacts weakly with the surrounding Fermi gas. The sign problem is worst in the crossover region when we are in between the two extreme cases. However, even there the sign problem remains quite manageable for the systems we have considered.

Having found evidence for a smooth crossover transition, we are now working on computing density correlations between up-spin particles and the down-spin impurity as well as the effective mass of the impurity. Both calculations should be straightforward using the ILMC method. This phenomenon of fermion/boson ambiguity for the impurities may have interesting consequences for systems of interacting impurities near the crossover transition. The ILMC approach is now also being applied to study impurities in paired superfluid systems, with applications to ultracold atomic systems and alpha particles in neutron gases.

Acknowledgements. We gratefully acknowledge illuminating discussions with C. Kollath, J. Levinsen, M. M. Parish, S. K. Baur, J. E. Thomas, T. Schäfer and S. Elhatisari. We also kindly thank M. Köhl, J. Ryckebusch and J. Vlietinck for sharing their data with us. Partial financial support was provided by the Helmholtz Association under contract HA216/EMMI, BMBF (grant 06BN9006), and U.S. Department of Energy (DE-FG02-03ER41260). This work was further supported by the EU (HadronPhysics3, Grant Agreement n. 283286). Computational resources were provided by the Jülich Supercomputing Centre at Forschungszentrum Jülich.

-
- [1] I. Bloch, J. Dalibard and W. Zwerger, *Rev. Mod. Phys.* **80** (2008) 885.
 - [2] N. V. Prokofev and B. V. Svistunov, *Phys. Rev. B* **77** (2008) 125101.
 - [3] N. V. Prokofev and B. V. Svistunov, *Phys. Rev. B* **77** (2008) 020408.
 - [4] F. Chevy and C. Mora, *Rep. Prog. Phys.* **73** (2010) 112401.
 - [5] C. Mora and F. Chevy, *Phys. Rev. A* **80** (2009) 033607.
 - [6] C. J. M. Mathy, M. M. Parish and D. A. Huse, *Phys. Rev. Lett.* **106** (2011) 166404.
 - [7] R. Combescot and S. Giraud, *Phys. Rev. Lett.* **101** (2008) 050404.
 - [8] R. Schmidt and T. Enss, *Phys. Rev. A* **83** (2011) 063620.
 - [9] S. Nascimbene *et al.*, *Phys. Rev. Lett.* **103** (2009) 170402.
 - [10] A. Schirotzek, C. H. Wu, A. Sommer and M. W. Zwierlein, *Phys. Rev. Lett.* **102** (2009) 230402.
 - [11] J. B. McGuire, *J. Math. Phys.* **7** (1966) 123.
 - [12] S. Zöllner, G. M. Bruun and C. J. Pethick, *Phys. Rev. A* **83** (2011) 021603.
 - [13] M. Klawunn and A. Recati, *Phys. Rev. A* **84** (2011) 033607.
 - [14] M. M. Parish, *Phys. Rev. A* **83** (2011) 051603.
 - [15] R. Schmidt, T. Enss, V. Pietilä and E. Demler, *Phys. Rev. A* **85** (2012) 021602(R).
 - [16] M. Koschorreck, D. Pertot, E. Vogt, B. Fröhlich, M. Feld and M. Köhl, *Nature*, **480** (2012) 619.
 - [17] Y. Zhang, W. Ong, I. Arakelyan and J. E. Thomas, *Phys. Rev. Lett.* **108** (2012) 235302.
 - [18] M. M. Parish and J. Levinsen, *Phys. Rev. A* **87** (2013) 033616.
 - [19] J. Vlietinck, J. Ryckebusch and K. Van Houcke, *Phys. Rev. B* **89** (2014) 085119.
 - [20] P. Kroiss and L. Pollet, *Phys. Rev. B* **90** (2014) 104510.
 - [21] N. V. Prokofev and B. V. Svistunov, *Phys. Rev. Lett.* **81** (1998) 2514.
 - [22] S. Elhatisari and D. Lee, *Phys. Rev. C* **90** (2014) 064001.
 - [23] D. Lee, *Phys. Rev. C* **78**, 024001 (2008).
 - [24] F. Chevy, *Phys. Rev. A* **74** (2006) 063628.
 - [25] Y. Shin, *Phys. Rev. A* **77** (2008) 041603.
 - [26] Y. Nishida and D. T. Son, *Phys. Rev. A* **75** (2007) 063617.
 - [27] H.-W. Hammer and D. Lee, *Phys. Lett. B* **681**, 500 (2009).
 - [28] L. He and P. Zhuang, *Phys. Rev. A* **78** (2008) 033613.
 - [29] G. J. Conduit, P. H. Conlon and B. D. Simons, *Phys. Rev. A* **77** (2008) 053617.
 - [30] J. Tempere, S. N. Klimin and J. T. Devreese, *Phys. Rev. A* **79** (2009) 053637.
 - [31] S. Yin, J. -P. Martikainen and P. Törmä, *Phys. Rev. B* **89** (2014) 014507.
 - [32] M. M. Parish and J. Levinsen, *Annual Review of Cold Atoms and Molecules: Volume 3*, World Scientific, Singapore (2015) [[arXiv:1408.2737](https://arxiv.org/abs/1408.2737) [cond-mat.quant-gas]].
 - [33] M. Köhl, talk at the 2012 APS March meeting.
 - [34] J. Levinsen, S. K. Baur, *Phys. Rev. A* **86** (2012) 041602.